

Burst-mode decision-feedback QPSK demodulator design

C. G. HIREMATH AND S. JAYASIMHA
Signion Systems Ltd, Hyderabad 500 082.
<http://www.signion.com>

Abstract

Numerical evaluation of the pdf's of a second-order DPLL's phase estimates is used to obtain phase-error distribution, phase variance, frequency offset estimator's bias and variance, cycle-slip and bit-error probability for a decision-feedback burst-mode QPSK demodulator (previous analyses consider only a first-order DPLL). This method also provides acquisition performance (in terms of maximum frequency offset acquired) when the transmitted bits are known (i.e. during preamble and/or unique words) as well as acquisition/tracking performance during data demodulation. A graphing method provides a means to obtain a good compromise between maximum frequency offset acquired (where large initial loop bandwidth is desired) and cycle-slip probability during the acquisition phase (where small-loop bandwidth is desired).

Keywords: Bandlimited signals, convergence of numerical methods, Costa's loops, digital demodulation, frequency estimation, satellite communications systems, signal processing, tracking loops.

1. Introduction

Burst-mode performance (where acquisition/pull-in time is a significant fraction of the burst duration) is typically optimized for a particular application and its associated parameters (burst duration and frequency offset). This is due to the trade-off among burst-mode acquisition time, maximum initial frequency offset to be acquired, preamble duration (bits known by the demodulator), phase error and consequent cycle-slip probability induced by decision feedback.

These trade-offs are addressed by an MPSK demodulator model (Section 2) which takes into account the presence of a frequency offset. The analysis of the model provides a series of graphs from which a designer may select preamble length and PLL parameters (including block size of a block-phase estimator) based on burst duration, maximum frequency offset to be acquired and maximum degradation of BER performance (at the operating E_b/N_0).

We extend the prior results¹ wherein a first-order Markov process is used to evaluate the performance of MPSK demodulator in the absence of frequency offset. That analysis,² while providing closed-form expressions, does not take into account systematic phase error due to frequency offset. We consider a second-order DPLL and, due to difficulties in obtaining closed-form expressions, use a numerical method to obtain graphs that aid a design space search. This numerical method allows the transient response of the DPLL to be observed as well.

¹When differential encoding is enabled the effect of cycle slip is to increase BER probability by about 10% in most operating E_b/N_0 's.

In general, large initial frequency offsets are present in many systems (where 'large' qualifies the ratio of carrier offset to bit rate, typically of the order of 0.1% or more). These offsets are introduced because carrier stability with inexpensive oscillators is at best 1 ppm. With carrier frequencies in the high GHz range, and considering that both transmitters and receivers have these offsets, at least a 50-kHz carrier offset is acquired. The large initial frequency offset is estimated from the burst's preamble to an accuracy the error limits of which can be tracked and corrected during demodulation. The residual frequency offset determines the loop bandwidth of the DPLL during acquisition, which in turn determines the performance of the DPLL.

The variance of acquired phase for different preamble lengths and E_b/N_0 's is provided in Section 3. While acquiring preamble, and during unique word demodulation, an estimate of the frequency offset can be derived (from differences in phase estimates). The probability of that residual frequency offset is halved after each demodulated block (for different block lengths) is examined in Section 4 (the designer may use the method described to obtain other graphs for different desired convergence rates).

Phase noise during tracking degrades BER performance. Section 5 shows that the phase noise variance, and consequently BER degradation is dependent on the length of the block-phase estimator. Another performance parameter, the cycle-slip probability, has significance when the differential decoder is disabled.^a Its dependence on block length and loop bandwidth is graphed in Section 6. Finally, Section 7 uses the graphs provided in Sections 3–6 to obtain design parameters of a QPSK demodulator, together with an illustrative example. Conclusions form Section 8.

2. System model

A feedback decision-directed phase-detector (DD-PD) MPSK demodulator (adapted from earlier work,^a with the first-order loop filter replaced by a second-order filter) is shown in Fig. 1.

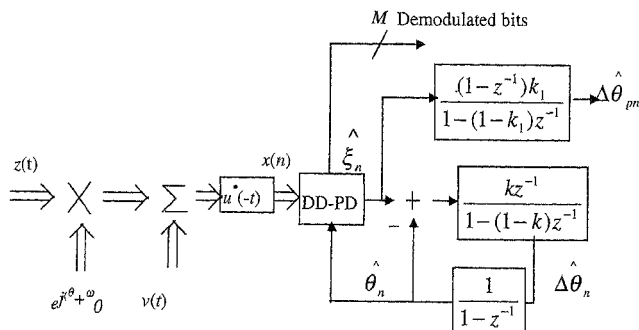


FIG. 1. MPSK demodulator system model.

The analytic baseband-transmitted signal $z(t)$ is

$$z(t) = \sqrt{E_s} \sum_{n=-\infty}^{\infty} e^{j\theta_T(n)} u(t - nT) \quad (1)$$

where $u(t)$ is the transmitted unit energy pulse shape, T the symbol time, $\theta_T(n)$ the transmitted phase of the n th symbol $\{\theta_T(n) = 2\pi i/M, i = 0, 1, \dots, M-1\}$ and E_s the energy per symbol. The transmitted pulse is assumed to satisfy Nyquist criterion for zero ISI. The channel corrupts the transmitted signal with additive white complex Gaussian noise and a multiplicative distortion (MD) $e^{j\theta_n + j\omega_b t}$. The MD represents the received phase θ_n and the frequency offset ω_b . It is assumed that large frequency offsets are corrected during carrier acquisition and the residual frequency offset is such that the phase offset due to frequency offset φ_{ω_d} ($\varphi_{\omega_d} = \omega_b t / f_{bd}$ and f_{bd} is the baud rate) is less than $\pi/(4MN_b)$ radians, where N_b is the block size (in symbols) for which phase is estimated. With known symbol timing at the receiver, the complex baseband signal at the output of the matched filter can be represented as

$$x_n = \sqrt{E_s} e^{j\psi_n} + v_n \quad (2)$$

where $\psi_n = \theta_T(n) + \theta_n + \varphi_{\omega_d} n$. The pdf of $\xi_n = \arg\{x_n\}$ for $N_b = 1$ is adapted from (3) of a prior work^a for MPSK modulations as

$$p_{\xi}(\xi_n | \psi_n) = \frac{e^{-(E_s/N_0)}}{2\pi} + \left[\frac{\sqrt{E_s}}{\sqrt{4\pi N_0}} \cos(\xi_n - \psi_n) e^{-(E_s/N_0) \sin^2(\xi_n - \psi_n)} \right] \left[1 + \operatorname{erf} \left(\frac{\sqrt{E_s}}{\sqrt{N_0}} \cos(\xi_n - \psi_n) \right) \right] \quad (3)$$

The pdf of $\hat{\xi}_n = \xi_n - \hat{\theta}_T(n)$ is used in the analysis of the synchronization subsystem and is given in (9) of Fitz and Cramer¹ as

$$p_{\hat{\xi}}(\alpha / \hat{\theta}_n, \psi_n) = \sum_{i=0}^{M-1} p_{\xi} \left(\alpha + \frac{2\pi i}{M} \mid \psi_n \right) \text{ for } \hat{\theta}_n - \frac{\pi}{M} \leq \alpha \leq \hat{\theta}_n + \frac{\pi}{M}, \quad M = 4 \text{ for QPSK} \\ = 0, \text{ elsewhere} \quad (4)$$

where $p_{\hat{\xi}}(\alpha / \psi_n)$ is expressed in eqn (3) of prior work.^a The angle α lies between the decision boundaries $\hat{\theta}_n - \pi/M$ and $\hat{\theta}_n + \pi/M$.

For $N_b > 1$, phase estimate, $\hat{\xi}_b$, for the block^b is

^aDigital implementation of a phase estimator involves a division and an arctangent table look-up. As these two operations are relatively expensive, the use of a block-phase estimator, in addition to reducing the variance of the phase estimate, also amortizes these two operations over the block length.

$$\hat{\xi}_b = \frac{\hat{\xi}_n + \hat{\xi}_{n+1} + \dots + \hat{\xi}_{N_b-1}}{N_b}. \quad (5)$$

The variance of $\hat{\xi}_b$ is less than the variance of $\hat{\xi}_n$ as it is the average of phase estimates of N_b symbols.^c As will be seen later, the block size determines the performance of the demodulator. The new phase estimate $\hat{\theta}_{n+1}$ and the averaged difference phase estimate $\Delta\hat{\theta}_{n+1}$ in the phase tracking loop are

$$\hat{\theta}_{n+1} = \hat{\theta}_n + (1-k)\Delta\hat{\theta}_{n-1} + k\{\hat{\xi}_b - \hat{\theta}_n\} \quad (6)$$

$$\Delta\hat{\theta}_n = (1-k)\Delta\hat{\theta}_{n-1} + k\{\hat{\xi}_b - \hat{\theta}_n\}. \quad (7)$$

The averaged difference phase estimate is the output of the first-order filter (the time constant of the filter is proportional to k). The new phase estimate $\hat{\theta}_{n+1}$ is equal to the sum of previous phase estimate and the averaged difference phase estimate. These two first-order filters constitute the loop filter of the DPLL and its overall response is second order (8). As a result, it tracks the phase variation due to frequency offset and the steady-state phase error is zero.

$$\hat{\theta}_{n+1} = (2-k)\hat{\theta}_n - (1-k)\hat{\theta}_{n-1} + k\{\hat{\xi}_b - \hat{\theta}_n\}. \quad (8)$$

k determines the behavior of the loop with frequency offset.

The difference in successive phase estimates is averaged using a single pole filter (with a time constant k_1) to obtain the difference phase estimate $\Delta\hat{\theta}_{pn}$ due to frequency offset

$$\Delta\hat{\theta}_{pn+1} = (1-k_1)\Delta\hat{\theta}_{pn} + k_1\{\hat{\xi}_b - \hat{\xi}_{b-1}\}. \quad (9)$$

3. Phase acquisition

As preamble symbols are known at the receiver, they can be used to estimate the phase of the signal. The pdf of the phase as given by (4) contains only one term corresponding to the preamble symbol which is evaluated numerically. Next, the individual-phase pdf's are convolved to obtain the overall pdf and hence the variance over a block. The plot of variance^d of phase for different block lengths N_b is shown in Fig. 2. It is seen that variance of phase σ_{ph}^2 decreases with increasing block length N_b . However, this improvement comes at a price: frequency offset tracked and block-length N_b are inversely related.

4. Frequency estimation using preamble and unique word

As each transmitter may have a different frequency offset, the receiver must reacquire the frequency offset for each burst. The preamble is used to find large frequency offsets^e using

^cThe variance approximately reduces by N_b as the pdf of the phase estimate is approximately gaussian for large SNRs.

^dThe phase distribution (in the absence of frequency offset) has zero mean (i.e. the pdf is symmetrical about 0°). However, pdf's are not symmetrical in the presence of frequency offset. The asymmetry increases with reducing SNR. However, this bias (which can also be numerically evaluated) is very small compared to phase variance and is therefore ignored.

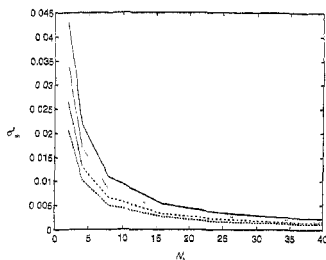


FIG. 2. Phase variance for different block lengths (with $k = 0.125$) after known bits are processed. Solid curve shows σ_{pn}^2 at 5 dB E_b/N_0 , '---' at 6 dB E_b/N_0 , '- · - · -' at 7 dB E_b/N_0 and the '—' curve at 8 dB E_b/N_0 .

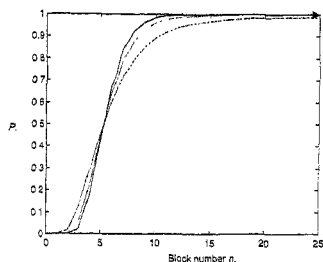


FIG. 3. Probability of frequency acquisition at different instants. The solid curve is for $N_b = 24$, '---' curve is for $N_b = 16$ and '- · - · -' curve is for $N_b = 8$.

spectral estimation techniques. During preamble and unique word demodulation, a single pole filter is used to obtain the estimate of the phase change $\Delta\hat{\theta}_{pn}$ due to frequency offset by averaging the differences in phase estimates. The pdf of $\Delta\hat{\theta}_{pn}$ is

$$p(\Delta\hat{\theta}_{pn+1} | \Delta\hat{\theta}_{pn}) = p\left((1-k_1)\Delta\hat{\theta}_{pn} + k_1\left\{\hat{\xi}_b - \hat{\xi}_{n-1}\right\}\right). \quad (10)$$

For QPSK, the maximum phase offset tolerable per block is $\pi/8$. Then, for phase and frequency offset estimation using preamble bits with a larger block length N'_b (for block-phase estimation), the error in the estimate of the frequency offset should be less than

$$f_{cr} = \frac{1}{16} \left(\frac{1}{N'_b} - \frac{1}{N_b} \right). \quad (11)$$

The probability, P_f , that the frequency correction is more than half of the original frequency offset for different block lengths N_b and for different preamble lengths⁷ is provided in Fig. 3 by numerically evaluating (10). This evaluation shows that asymptotic convergence improves with block length at the expense of initial convergence rate which justifies the use of different block lengths at different acquisition stages.

⁷For MPSK, the preamble is an unmodulated carrier which allows reliable acquisition of large frequency offsets at poor SNR using a periodogram.

⁸More effective use of the unmodulated carrier can be made by overlapping and periodogram averaging, reducing the variance of the estimated frequency offset. The reduction in phase variance using a Gaussian approximation (valid for high SNRs) (see 8.1.38) of Proakis *et al.*²). This improvement, usually taken advantage of in practical QPSK demodulators, merely reduces the preamble length by the overlapping factor (provided that the factor is ≤ 2).

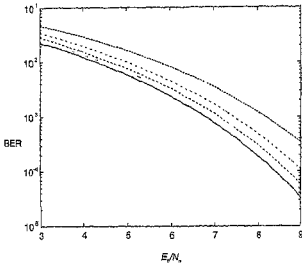


FIG. 4. BER performance for different block lengths. Solid curve shows theoretical performance, '---' curve is for $N_b = 16$, '-----' curve is for $N_b = 8$, '- · - · -' curve is for $N_b = 4$ and the '·····' curve is for $N_b = 2$.

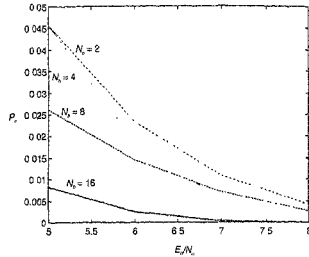


FIG. 5. Probability of cycle slip for different block lengths with frequency offset equal to bit rate/(16 N_b) and with $k = 0.125$.

5. BER degradation

Modern BER degrades with increased phase estimation error. For QPSK, the degradation is estimated by comparing the performance curves obtained using (26) of prior work¹ with phase estimation error (which includes the systematic error due to frequency offset) and without any phase error (i.e. with $\phi = 0$).

$$P_B(E/\phi) = \frac{1}{4} \operatorname{erfc} \left[\sqrt{\frac{E_b}{N_o}} (\cos \phi - \sin \phi) \right] + \frac{1}{4} \operatorname{erfc} \left[\sqrt{\frac{E_b}{N_o}} (\cos \phi + \sin \phi) \right] \quad (12)$$

Figure 4 shows burst-mode BER vs E_b/N_o 's in dB for various block lengths⁸ and reiterates the results of Fig. 2 in the light of (12) from a different viewpoint (i.e. BER degradation is caused by phase error). These curves may be used to find a block length that yields an optimal trade-off between frequency offset⁸ tracked and BER degradation (Figure 4 is of greater practical interest than Fig. 2 as BER degradation is more easily measured than phase variance).

6. Cycle-slip performance

For QPSK, stable phase states are 0° , $\pm 90^\circ$ and 180° with reference to carrier phase. The initial phase $\hat{\theta}_0$ estimated from preamble¹ is close to the 0° stable state from the carrier phase. When cycle slip occurs, phase $\hat{\theta}_n$ is near other stable states and the probability that it relocks

⁸In prior work,¹ ϕ is chosen such that BER at 6.0 dB E_b/N_o is degraded by 0.5 dB. A more accurate estimate of BER, and hence the degradation may be obtained by numerically integrating the product of (12) and the numerically evaluated pdf of ϕ .

⁹Even for continuous mode operation, it is desirable to use a finite length for the block-phase estimator as the steady-state frequency offset is non-zero (due to relative motion and clock drifts).

¹⁰The constant preamble pattern for QPSK should be such that the in-phase bit is the complement of the quadrature bit.

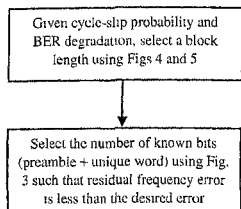


FIG. 6. Selection of QPSK demodulator parameters.

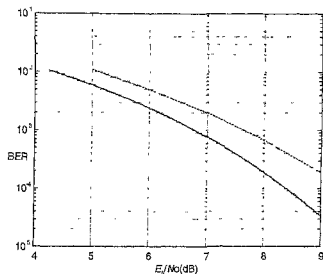


FIG. 7. Burst-mode performance of the QPSK modem in AWGN (solid curve represents theoretical performance and broken curve the designed modem)

to the 0° stable state is small. Therefore, cycle slip is likely when $\hat{\theta}_n$ changes by more than 45° for QPSK. The cycle-slip probability is given by the cumulative probability that the next phase estimate changes by more than 45° . This probability depends on $p(\hat{\theta}_n | \hat{\theta}_{n-1}, \hat{\theta}_{n-2})$ as can be seen from (8).

Figure 5 shows the theoretical probability that $\hat{\theta}_n$ changes by more than 45° (i.e. cycle-slip probability) for different E_b/N_0 and block length with maximum frequency offset (these curves were obtained by numerically evaluating (8)).

7. Design of QPSK demodulator parameters

A simple non-iterative two-step procedure to select a QPSK demodulator's parameters is depicted in Fig. 6.

For example, suppose that the bit rate is 8.192 Mbps and the maximum frequency offset is 50 kHz, of which, assume that residual frequency offset after using 50% overlap spectral estimation referred to in Section 4 (using only the unmodulated carrier of 48 bits) is 24 kHz. Next, assume that cycle-slip probability for any early demodulated block (where the cycle-slip probability is high due to the use of short blocks to acquire residual frequency offset) is required to be less than 0.01 at $E_b/N_0 = 5$ dB. Further, suppose that the BER degradation permitted (over a 2400-bit burst) is 0.5 dB as compared to continuous-mode operation.

From Figs 4 and 5, $N_b = 16$ is a reasonable compromise. From Fig. 3, the number of known bits should be at least 64 (i.e. there must be at least 16 bits of unique word) so that the probability that the residual frequency offset is further halved is greater than 0.7 (we can use six 50% overlapped blocks of 16 bits each). However, the unique word length is usually selected on other considerations (probability of false alarm), and usually a 24- or 32-bit unique word is used. For a 32-bit unique word, the total known bits (preamble + unique word) is 96 and for a 2400-bit burst, the effective payload reduction is 4%.

Table I
Probability of cycle slip

E_p/N_0	Probability of cycle slip
5	0.0588
6	0.0392
7	0
8	0

An 8.192-Mbps system was simulated in MATLAB based on chosen parameters. The results of the simulation^k (Fig. 7 and Table I) were slightly worse (by 0.3 dB) than the results predicted by the graphs provided. The error is attributed to sampling in the matched filter, frequency estimation error, synchronization error, etc. which are not taken into consideration by the graphs provided (as these are determined by other practical system design considerations).

8. Conclusions

Numerical evaluation of phase distribution provides performance predictors for a decision-directed feedback DPLL QPSK demodulator. The following conclusions can be drawn from this analysis:

- Increasing preamble duration reduces residual frequency offset (see Fig. 3) almost inversely.
- Cycle-slip probability and BER degradation determine the block length and also the payload reduction for a burst demodulator.
- At lower E_p/N_0 's the preamble length must be increased reducing the effective payload of the burst significantly.^l
- Even though new coding schemes and decoding methods promise continuous-mode operation at E_p/N_0 's significantly lower than 5 dB, frequency offset acquisition and tracking in burst mode will require larger implementation margins (either in terms of reduced payload or increased transmitted power).

Design parameters of QPSK demodulators can be chosen using these performance predictors.

References

1. FITZ, R. D. AND CRAMER, R. J.-M. A performance analysis of a digital PLL-based MPSK demodulator, *IEEE Trans.*, 1995, C-43, 1192-1201.
2. PROAKIS, J. G., RADER, C. M., LING, F. AND NIKIAS, C. L. *Advanced digital signal processing*, Macmillan, 1992, pp. 479-484

^kHere we note that the number of bits of unique word that are allowed to be in error is increased beyond minimal requirement to meet the probability of missed detection, as these bits will have a poorer error rate due to high residual frequency offset.

^lResults shown in Fig. 7 and Table I correspond to burst duration of 2,400 bits (including preamble and unique word). BER and cycle-slip probability for burst mode is obtained by averaging the bit errors and cycle clips over N bursts (where $N > 100$ for all E_p/N_0 's) using a uniform distribution of frequency offsets between -50 and +50kHz.

^mBurst duration is designed based on multiple access considerations (such as traffic characteristics, number of users, maximum delay, etc.) and cannot usually be increased to enhance payload.